Computing costs of imaging for the xNTD

T.J. Cornwell, ATNF

Tim.Cornwell@csiro.au

10/2/06

Abstract: *I investigate the computing costs of imaging for an SD+FPA telescope such as the xNTD or KAT by conducting simulations of continuum and spectral line imaging. I find that the spectral line imaging costs dominate by many orders of magnitude. For antennas with equatorial mounts, the computing load is about 20TFlops. With Moore's Law and possible algorithmic improvements, a plausible hardware cost lies in the range A$2M to A$4M (2009). Equatorial mounts are cost effective in controlling computing costs since with current algorithms the processing for alt-azimuth is at least a factor of 3 – 4 more expensive. Computing costs for a Big Gulp solution are half those of the SD+FPA with equatorial mounts.*

1. Introduction

This note follows on from Cornwell (2005), in which I examined the case to be made for a LNSD design for SKA stations. In this note, I concentrate on the computing costs for a SD+FPA system – specifically a possible configuration for the xNTD. The goal of the work reported here is to make a first estimate of the computing costs for imaging with such a system.

I have repeated refined versions of the simulations previously reported, this time focusing on the scale of the computing required. This work was made possible by the acquisition of a large memory Opteron-based server *(delphinus)* at the ATNF running a 64 bit capable version of AIPS++.

2. Review of imaging

An interferometer measures the visibility function, multiplied by the far field voltage pattern of the two antennas:

$$V_{ij,p} = \int E_{i,p}(l,m) E^{*}_{j,p}(l,m) I(l,m) e^{2\pi i \left(u_{i,j} l + v_{i,j} m + w_{i,j} \sqrt{1-l^2-m^2} \right)} dldm$$

Equation 1

Assuming that all antennas have the same voltage pattern for a point *p:*

$$V_{ij,p} = \int A_p(l,m) I(l,m) e^{2\pi j\left(u_{i,j}l + v_{i,j}m + w_{i,j}\sqrt{1-l^2-m^2}\right)} dldm$$

Equation 2

The power pattern is given by:

$$A_p(l,m) = \left|E_p(l,m)\right|^2$$

Equation 3

Suppose that we form dirty images from the measured visibilities by the standard process. We can then form an optimum estimate of the sky from a "linear mosaic" of the dirty images:

$$I^{LM}(l,m) = \frac{\sum_p A_p(l,m) I_p^D(l,m)}{\sum_p A_p{}^2(l,m)}$$

Equation 4

For spectral line imaging where the continuum has been subtracted by some means, often this linear mosaic will suffice as a good estimate of the sky.

For continuum imaging, an iterative process is followed. A model of the sky is constructed. The predicted model visibility function is calculated by evaluation of equation (1). The residual visibility (observed minus model) is then used to calculate a residual linear mosaic image. This is then cleaned, using an approximate point spread function, and the process iterated. Thus many forward (model image to model visibility) and backwards (residual visibility to residual image) steps are required.

The approximate point spread function may be estimated as follows. If the individual point spread functions $B_p(l,m)$ are identical (a good approximation for a focal plane array enabled telescope), then an approximate convolution equation holds:

$$I^{LM}(l,m) \approx B^{LM}(l,m) * I(l,m)$$

Equation 5

The effective (linear mosaic) point spread function is given by:

$$B^{LM}(l,m) = B(l,m)\frac{\sum_p A_p(l,m)A_p(l=0,m=0)}{\sum_p A_p{}^2(l,m)}$$

Equation 6

An alternative approach is possible – the data from the individual pointings p are deconvolved separately and then combined via a linear mosaic. This is common practice at the ATCA and works well if the pointing positions do not move on the sky (as would occur for a focal plane array on alt-azimuth mounted antennas).

The computationally expensive steps in the processing are:

- Gridding the visibility data onto a regular grid for subsequent Fourier transform. This must include correction for the *w*-term. The reverse step is to degrid to obtain estimates at the irregular sample points.
- Inverse Fourier transformation to the image plane, or Fourier transformation to the *uv* space.
- Multiplication by the primary beam.

These steps have to be partitioned according to the constancy of the various terms. For example, the multiplication by the primary beam needs to be done for each different primary beam, thus incurring more Fourier transforms. The gridding/degridding costs are more or less independent of the primary beam.

3. Simulations

The simulations used a model of the 1.5GHz continuum sky described by Cornwell (2005):

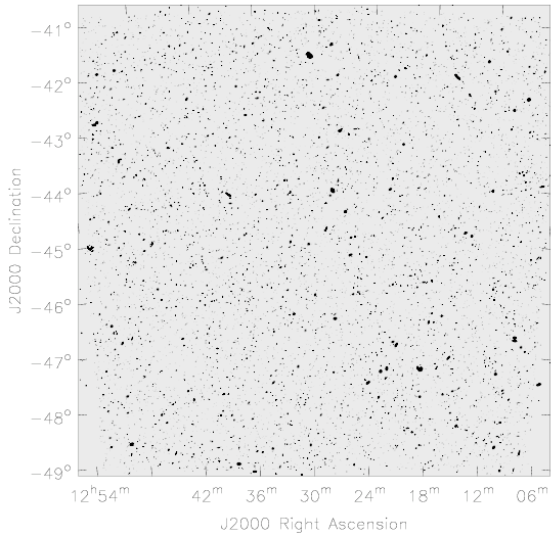

Figure 1 Model image for simulations

In Table 1, I show the simulations performed and the derived numbers.

- The SDFPA antennas were 15m diameter (2m blockage) equatorial mount.
- Two configurations were used: for the first, the antenna layout was optimized for a single frequency 1 hour integration using Boone's (2001) method, and for the second, a three-armed spiral layout was optimized "by eye" for multi-frequency synthesis.

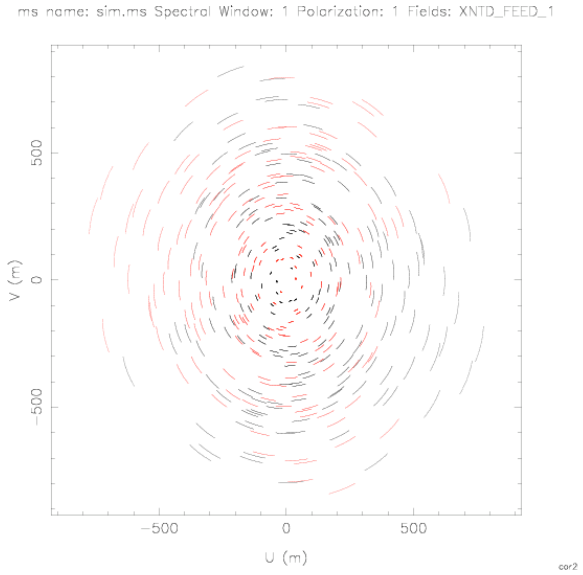

Figure 2 SDFPA configuration 1

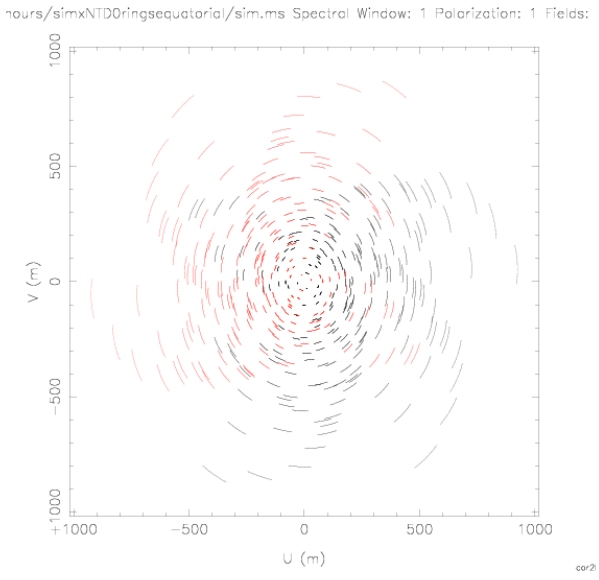

Figure 3 SDFPA configuration 2

- The feeds were arranged in hexagons of varying number of rings. The maximum

was 4 rings, giving 61 feeds. The feeds were critically sampled – at half a wavelength.

- The feed voltage patterns are assumed to be sufficiently azimuthally symmetric that if the feed were on axis, correction as a function of parallactic angle would not be required. This is not obviously true, at least for continuum imaging.
- Two sets of simulations were performed – continuum and spectral line. For continuum imaging, 8 channels were imaged with 60 seconds integration time. For spectral line, these numbers were multiplied by 4, thus keeping the data volume roughly constant.
- The total integration time for both cases was 1 hour.
- A joint clean of the entire field of view was used for the continuum image since a joint clean will be necessary for alt-azimuth antennas. The spectral line data was also cleaned. The continuum was removed by subtracting that model from the visibilities and a residual image formed from that data.
- W projection is needed to correct the non-coplanar baselines effect for the large fields of view encountered here.
- I timed the various steps by the wall clock. For all cases, the processing was CPU limited.
- The number of processors is calculated by scaling to the full observation. For the continuum case, there is no scaling – the simulation is of the full observation. The number of processors is derived from the cleaning costs. For the spectral line case, I scale from the time taken to calculate the residual cube image from the continuum subtracted data *i.e.* we assume that cleaning is not required for most channels.
- The computing configuration was a Sun v20Z, dual dual-core Opteron 275 processors, 1MB cache, 8GB memory, with two UltraSCSI disks, running AIPS++ version 19.1270, optimized using GCC 3.3.4 –O2 option. This computer cost about A$13,000 (roughly US$10,000) in October 2005.
- The Big Gulp configuration is of 220 antennas of 4.5meter diameter with single feeds. The antenna size has been increased compared to Cornwell (2005) to match the field of view of the three ring SDFPA.

Table 1 Simulation summary. Lines in yellow mark the canonical 37 feed configuration. The cycles per visibility measure the number of Opteron 275 cycles to process a visibility. The cost is scaled from the 2005 price of the server.

Config	Mode	Mount	Nant	Baseline	Feeds	Chan	Nint	t	Nvis	Clean	Residual	Clean	Residual	Data	Req chan	Proc	Cost (2005)	Data rate
				(m)				(sec)		(sec)		(cycles/vis)		(GB)			A$M	(GB/hour)
1	Continuum	equatorial	21	1100	1	8	60	60	100800	54		1.2E+06		0.01	8	0.02	0.00	0.01
2	Continuum	equatorial	20	1000	1	8	60	60	91200	63		1.5E+06		0.01	8	0.02	0.00	0.01
1	Continuum	equatorial	21	1100	7	8	60	60	705600	167		5.2E+05		0.08	8	0.05	0.00	0.08
1	Continuum	alt-az	21	1100	7	8	60	60	705600	1345		4.2E+06		0.64	8	0.37	0.00	0.64
2	Continuum	equatorial	20	1000	7	8	60	60	638400	138		4.8E+05		0.07	8	0.04	0.00	0.07
2	Continuum	alt-az	20	1000	7	8	60	60	638400	1453		5.0E+06		0.76	8	0.40	0.00	0.76
1	Continuum	equatorial	21	1100	19	8	60	60	1915200	455		5.2E+05		0.22	8	0.13	0.00	0.22
2	Continuum	equatorial	20	1000	19	8	60	60	1732800	499		6.3E+05		0.07	8	0.14	0.00	0.07
2	Continuum	alt-az	20	1000	19	8	60	60	1732800	3790		4.8E+06		0.21	8	1.05	0.00	0.21
1	Continuum	equatorial	21	1100	37	8	60	60	3729600	811		4.8E+05		0.42	8	0.23	0.00	0.42
2	Continuum	equatorial	20	1000	37	8	60	60	3374400	997		6.5E+05		0.38	8	0.28	0.00	0.38
1	Continuum	equatorial	21	1100	61	8	60	60	6148800	3593		1.3E+06		0.69	8	1.00	0.00	0.69
2	Continuum	equatorial	20	1000	61	8	60	60	5563200	4668		1.8E+06		0.62	8	1.30	0.00	0.62
Big gulp	Continuum	alt-az	220	1100	1	8	60	60	92505600	283		6.7E+03		1.28	8	0.08	0.00	1.28
1	Spectral	equatorial	21	1100	1	32	15	240	100800	52	71	1.1E+06	1.5E+06	0.01	65536	161.56	0.48	81.92
2	Spectral	equatorial	20	1000	1	32	15	240	91200	49	67	1.2E+06	1.6E+06	0.01	65536	152.46	0.46	81.92
1	Spectral	equatorial	21	1100	7	32	15	240	705600	184	348	5.7E+05	1.1E+06	0.07	65536	791.89	2.38	573.44
1	Spectral	alt-az	21	1100	7	32	15	240	705600	1507	1379	4.7E+06	4.3E+06	0.06	65536	3137.99	9.41	491.52
2	Spectral	equatorial	20	1000	7	32	15	240	638400	175	520	6.0E+05	1.8E+06	0.07	65536	1183.29	3.55	573.44
2	Spectral	alt-az	20	1000	7	32	15	240	638400	1059	1184	3.6E+06	4.1E+06	0.07	65536	2694.26	8.08	573.44
1	Spectral	equatorial	21	1100	19	32	15	240	1915200	483	2062	5.5E+05	2.4E+06	0.2	65536	4692.20	14.08	1638.40
2	Spectral	equatorial	20	1000	19	32	15	240	1732800	474	1598	6.0E+05	2.0E+06	0.2	65536	3636.34	10.91	1638.40
2	Spectral	alt-az	20	1000	19	32	15	240	1732800	1598	6591	2.0E+06	8.4E+06	0.19	65536	14998.19	44.99	1556.48
1	Spectral	equatorial	21	1100	37	32	15	240	3729600	771	2404	4.5E+05	1.4E+06	0.39	65536	5470.44	16.41	3194.88
2	Spectral	equatorial	20	1000	37	32	15	240	3374400	938	2344	6.1E+05	1.5E+06	0.35	65536	5333.90	16.00	2867.20
1	Spectral	equatorial	21	1100	61	32	15	240	6148800	2793	11300	1.0E+06	4.0E+06	0.64	65536	25713.78	77.14	5242.88
2	Spectral	equatorial	20	1000	61	32	15	240	5563200	4522	11344	1.8E+06	4.5E+06	0.58	65536	25813.90	77.44	4751.36
Big gulp	Spectral	alt-az	220	1100	1	32	15	240	92505600	283	1184	6.7E+03	2.8E+04	1.2	65536	2694.26	8.08	9830.40

In the following images, I show the continuum images for the two SD+FPA configurations with the canonical three rings of feeds and the Big Gulp configuration.

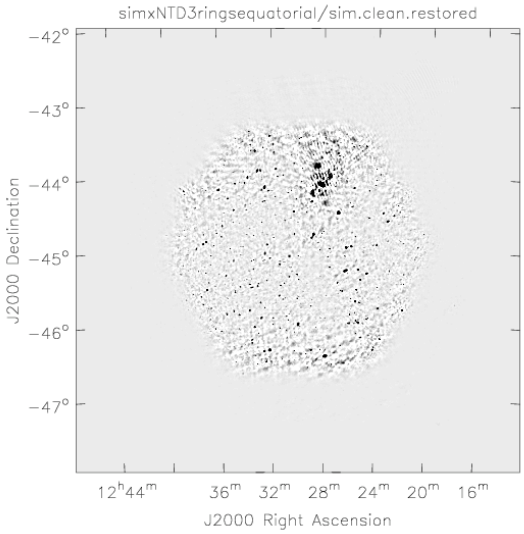

Figure 4 SDFPA configuration 1. Display range -1 to 10mJy/beam.

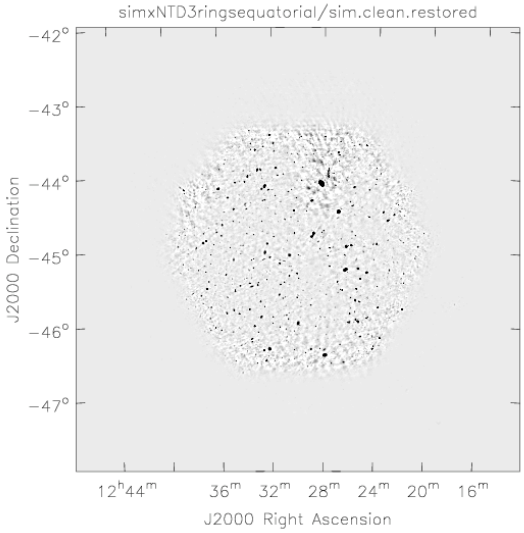

Figure 5 SDFPA configuration 2. Display range -1 to +10mJy/beam.

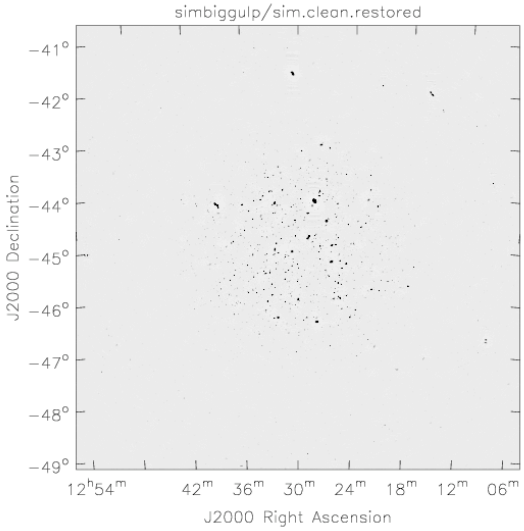

Figure 6 Big gulp image. Display range -1 to 10 mJy/beam.

4. Discussion

The spectral line case dominates both processing and data costs by huge factors. The canonical case of an array of twenty equatorially mounted antennas with 37 feeds arranged in 3 rings, requires about 5000 processors to keep up with full resolution spectral line observing (assuming 100% efficiency). Scaling from a number of machines on the Top 500 list (http://www.top500.org), this corresponds to a maximum performance of about 20TFlops. The total computing capital cost (2005) to sustain the full data rate all the time with current software is about A$15M. The budgeted cost (2009) should be

some fraction of this number – A$2M to A$4M - because of (a) Moore's Law, (b) expected software and methodological improvements and (c) the likely mixture of science requiring fewer channels.

Since the processing for spectral line observing is likely to drive the computing costs, we can afford much more sophisticated processing for the continuum case. This may be necessary to cope with, for example, the non-ideal FPA primary beams.

Since embarrassingly parallel processing will be required for spectral observations, the processor interconnection bandwidth need not be very large. This will be considerably cheaper and easier to develop than parallel processing for continuum imaging where high interconnection bandwidth may be required, especially if the continuum processing is significantly more involved than that simulated here. It may make sense to have multiple computational facilities, dedicated to different science – continuum or spectral line, for example.

Processing for alt-azimuth telescopes is more demanding computationally since the pointing locations rotate on the sky with hour angle, necessitating a larger number of operations. The data for a given feed are binned into time chunks for which the beam location is approximately constant. This multiplies the number of voltage pattern applications and Fourier transforms correspondingly but the gridding and degridding operations remain the same. The simulations show that with current algorithms, implementing SD+FPA with alt-azimuth mounts would increase the processing cost by a factor of at least 3 to 4. Hence equatorial mounts are very likely to be cost-effective.

The data rate is independent of the mount choice. The highest data rate is roughly a few TB per hour. Assuming a cost for storage of about $100/TB (an optimistic number for 2009) and that we operate at full spectral resolution, the annual disk storage cost to keep the data would be about A$250K. The AIPS++ model is to keep separate copies of the observed, calibrated, and model data. Thus the costs could be reduced down to about A$100K per annum by re-computing the latter two as needed.

5. Recommendations

- The xNTD should continue to investigate costs of an equatorial mount for the xNTD antennas.
- Algorithmic work should concentrate on improving the efficiency of primary beam application for alt-az mounts. There is a lot of latitude to restructure the algorithms to minimize computing costs. For example, the primary beams can be applied as convolutions in Fourier space at the same time the *w*-term is corrected (Bhatnagar *et al.,* 2005).
- The first priority in parallelization must be to develop a framework for parallel processing of spectral line data, including calibration and continuum subtraction. Parallel algorithms for high dynamic range continuum imaging can take second priority.
- We should spend some more effort to optimize the Fourier plane coverage of the

xNTD. The better of the two SDFPA configurations used here, the second, is probably still quite sub-optimal, as evidenced by the continuum image quality, especially compared to Big Gulp. Boone's method can be extended to allow explicitly for MFS, which must be taken into account for designing an array with a relatively small number of antennas.

The actual numbers in this memo are still quite subject to change under different assumptions for the processing. Continuing refinement of these simulations is advisable. In particular, we should investigate whether it is true that the processing for spectral line data is as straightforward as assumed here. If this assumption holds, we can expect to be able to predict the overall computing load with good accuracy prior to operations.

Acknowledgements

I thank Vince McIntyre and Shaun Amy for acquiring and commissioning *delphinus,* the 64 bit server used. I thank Frederic Boone for making available the APO source code for his array optimization method.

References

Bhatnagar, S., Cornwell, T.J., and Golap, K., 2004, EVLA memo 84, see http://www.aoc.nrao.edu/evla/memolist.html.

Boone, F., 2001, A&A, **377**, 368-376.

Cornwell, T.J., 2005, SKA memo 61, see http://www.skatelescope.org.